

# The role of $D_0^{**}$ in $B^- \rightarrow D_s^+ K^- \pi^-$

Oleg Antipin and G. Valencia\*

*Department of Physics and Astronomy,  
Iowa State University,  
Ames, IA 50011*

(Dated: December 2, 2024)

## Abstract

The BaBar collaboration has recently reported the observation of the decay mode  $B^- \rightarrow D_s^+ K^- \pi^-$ . We investigate the role played by the  $D^{**}$  resonances in this decay mode using HQET. Although these resonances cannot appear as physical intermediate states in this reaction, their mass is very close to the  $D_s^+ K^-$  production threshold and may, therefore, play a prominent role. We pursue this possibility to extract information on the properties of the strong  $D^{**}DM$  couplings. As a byproduct of this analysis we point out that future super- $B$  factories may be able to measure the  $D_0^0 D^* \gamma$  radiative coupling through the reaction  $B^- \rightarrow D^* \gamma \pi^-$ .

---

\*Electronic address: oaanti02@iastate.edu; valencia@iastate.edu

## I. INTRODUCTION

The BaBar collaboration has recently reported the observation of the decay mode  $B^- \rightarrow D_s^+ K^- \pi^-$  with a branching ratio  $\mathcal{B}(B^- \rightarrow D_s^+ K^- \pi^-) = (1.88 \pm 0.13 \pm 0.41) \times 10^{-4}$  [1]. This decay mode is different from the mode  $B^- \rightarrow D^{**} \pi^- \rightarrow D^+ \pi^- \pi^-$  observed by Belle [2] in that the  $D^{**}$  resonances are too light to decay into  $D_s^+ K^-$ . Nevertheless their masses [2],

$$\begin{aligned} m_{D_0^{**}} &= (2308 \pm 17 \pm 15 \pm 28) \text{ MeV} \\ m_{D_2^{**}} &= (2461.6 \pm 2.1 \pm 0.5 \pm 3.3) \text{ MeV}, \end{aligned} \quad (1)$$

are sufficiently close to the threshold for production of  $D_s^+ K^-$  that we can entertain the possibility of them playing a significant role in  $B^- \rightarrow D_s^+ K^- \pi^-$  as “quasi-resonant” intermediate states.

In this paper we use heavy quark effective theory (HQET) to investigate this possibility. This study will serve as a probe of the properties of the  $D^{**}DM$  interactions, where  $M$  a member of the light pseudoscalar meson octet. In particular we can check the  $SU(3)$  relations in strong  $D^{**}$  decay. In addition, an analysis of a distribution with respect to the angle between the pion and kaon momenta can further constrain the  $D_s^0$  tensor couplings.

Schematically, our procedure consists of splitting the decay  $B^- \rightarrow D_s^+ K^- \pi^-$  into “quasi-resonant” and non-resonant contributions as depicted in Figure 1. If

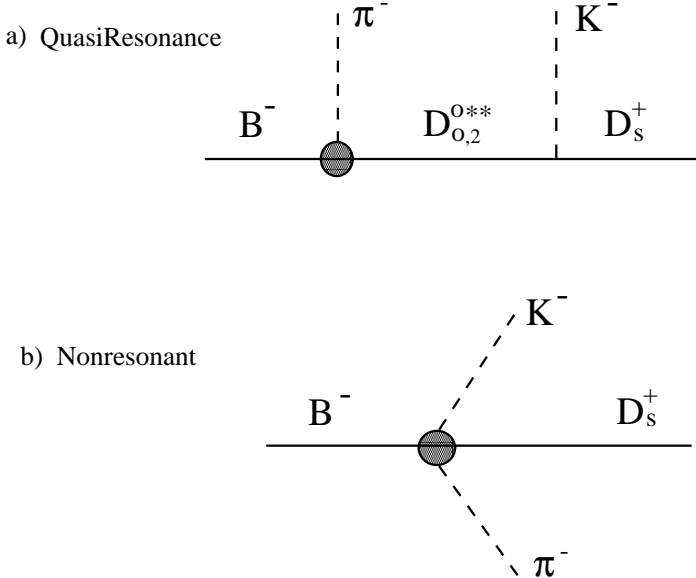


FIG. 1: Decomposition of the decay mode  $B^- \rightarrow D_s^+ K^- \pi^-$  into contributions that are mediated by a  $D^{**}$  that is near its mass shell and those that are not.

the  $D^{**}$  resonances were heavy enough to decay into  $D_s^+ K^-$  we would expect the

“quasi-resonant” contribution to dominate. Furthermore, in the narrow width approximation the production and decay processes would factorize, and we could study the properties of the strong decay vertex. We investigate the extent to which the “quasi-resonant” process dominates by first computing the amplitudes with the aid of heavy quark effective theory (HQET). We then normalize the resulting rates to the two-body  $B^- \rightarrow D_{0,2}^0 \pi^-$  weak decay rates and this will serve as a constraint on the weak transition. Finally we study the behavior of the normalized rates for different parametrizations of the weak vertex, treating the residual dependence on the weak vertex as an indication of the extent to which the “quasi-resonant” contribution dominates.

## II. FORMALISM

We use the HQET formalism to describe the interactions involving the heavy meson  $(0^-, 1^-)$  doublet, its excited positive parity partners  $(0^+, 1^+)$  and  $(1^+, 2^+)$ , and light pseudo-scalar mesons [3, 4, 5, 6, 7, 8]. We follow standard notation to incorporate the light pseudo-scalars as the Goldstone bosons of spontaneously broken chiral symmetry through the matrix  $\xi = \exp(\frac{iM}{f_\pi})$  with a normalization in which the pion decay constant is  $f_\pi = 132$  MeV. The matrix  $M$  is explicitly given by,

$$M = \begin{pmatrix} \sqrt{\frac{1}{2}}\pi^0 + \sqrt{\frac{1}{2}}\eta & \pi^+ & K^+ \\ \pi^- & -\sqrt{\frac{1}{2}}\pi^0 + \sqrt{\frac{1}{6}}\eta & K^0 \\ K^- & \bar{K}^0 & -\sqrt{\frac{2}{3}}\eta \end{pmatrix}. \quad (2)$$

Similarly, the heavy meson doublets are described by the following fields and their conjugates,

$$\begin{aligned} (0^-, 1^-) &\rightarrow H = \frac{1+\psi}{2}(H^* - P\gamma_5), \bar{H} = \gamma_0 H^\dagger \gamma_0 \\ (0^+, 1^+) &\rightarrow S = \frac{1+\psi}{2}(P_1\gamma_5 - P_0), \bar{S} = \gamma_0 S^\dagger \gamma_0 \\ (1^+, 2^+) &\rightarrow T^\mu = \frac{1}{2}(1+\psi) \left[ P_2^{\mu\nu} \gamma_\nu - \sqrt{3/2} \tilde{P}_{1\nu} \gamma_5 (g^{\mu\nu} - \frac{1}{3}\gamma^\nu(\gamma^\mu - v^\mu)) \right], \\ &\bar{T}^\mu = \gamma_0 T^{\dagger\mu} \gamma_0. \end{aligned} \quad (3)$$

At leading order in the heavy quark and chiral expansions, the strong interaction mediated decays of the form  $H, S, T \rightarrow HM$  are described by the Lagrangians [3, 4, 5, 9]

$$\begin{aligned} \mathcal{L}_H &= g \operatorname{Tr} [H \gamma_\mu \gamma_5 A^\mu \bar{H}], \\ \mathcal{L}_S &= h \operatorname{Tr} [S \gamma_\mu \gamma_5 A^\mu \bar{H}] + \text{h.c.}, \\ \mathcal{L}_T &= \frac{h_1}{\Lambda_\chi} \operatorname{Tr} [H \gamma_\lambda \gamma_5 (D_\mu A^\lambda) \bar{T}^\mu] + \frac{h_2}{\Lambda_\chi} \operatorname{Tr} [H \gamma_\lambda \gamma_5 (D^\lambda A_\mu) \bar{T}^\mu] + \text{h.c.}, \end{aligned} \quad (4)$$

where the axial current is given by,

$$A_\mu \equiv \frac{i}{2}(\xi^\dagger \partial_\mu \xi - \xi \partial_\mu \xi^\dagger), \quad (5)$$

and the traces are over Dirac and flavor indices. For our numerical estimates we will use the values  $|h'| = |(h_1 + h_2)/\Lambda_\chi| \approx 0.5 \text{ GeV}^{-1}$ ,  $h = -0.52$  and  $g = 0.4$  [8, 10]. We will also replace  $f_\pi \rightarrow f_K \sim 1.3 f_\pi$  where appropriate.

It is a simple exercise to write the corresponding weak vertices describing the transitions from a  $b$ -quark meson to a  $c$ -quark meson. In this case, however, we do not expect a reliable description of the weak transition as the  $m_b - m_c$  mass difference is larger than  $\Lambda_\chi$ . We will use the HQET framework to parametrize the weak transitions in a manner similar to that of Ref. [11]. We then treat the result as a phenomenological description of the weak transition in terms of three free parameters that are constrained by the two body decays  $B^- \rightarrow D_{0,2}^0 \pi^-$ .

The dominant short distance operator responsible for the decays  $B^- \rightarrow D_s^+ K^- \pi^-$ ,  $B^- \rightarrow D^+ \pi^- \pi^-$  is an  $SU(3)$  octet of the form  $\bar{c}\gamma_\mu(1 - \gamma_5)b\bar{d}\gamma^\mu(1 - \gamma_5)u$ . We use standard techniques [12] to introduce this operator into the HQET formalism. We first construct the matrix  $h$  with  $h_j^i = \delta_1^i \delta_j^2$  to represent the  $SU(3)$  properties of the operator. We then pretend that  $h$  transforms as  $h \rightarrow LhL^\dagger$  under chiral symmetry and construct chiral symmetric operators that include  $h$ . The transformation properties under chiral symmetry of the other relevant objects are  $H_Q \rightarrow H_Q U^\dagger$ ,  $\bar{H}_Q \rightarrow U \bar{H}_Q$ ,  $\xi \rightarrow L\xi U^\dagger$  and  $\xi^\dagger \rightarrow U \xi^\dagger L^\dagger$ . With these ingredients we construct the effective weak Lagrangian beginning with the  $H_b \rightarrow H_c$  transitions. There is only one term without derivatives (the sign is chosen to match the notation in [13]),

$$\mathcal{L}_W = -\beta'_W \text{Tr} [ H_b \xi^\dagger \gamma_\mu(1 - \gamma_5) h ] \text{Tr} [ \xi \bar{H}^c \gamma^\mu(1 - \gamma_5) ]. \quad (6)$$

There is also a unique term with one derivative,

$$\mathcal{L}_{W1} = ik_H \text{Tr} [ H_{bj} \bar{H}^{cj} \gamma_\mu(1 - \gamma_5) ] \text{Tr} [ \xi^\dagger h \partial^\mu \xi ]. \quad (7)$$

Even though the operator Eq. 7 is formally suppressed by one order in the momentum expansion with respect to the one in Eq. 6 we will keep both of them for several reasons. First, because in a matching to the underlying quark-operator Eq. 6 is suppressed by  $1/N_c$  with respect to Eq. 7; second, because we do not really expect the momentum expansion to be relevant in  $b \rightarrow c$  transitions; and third, because Ref. [11] finds that an interplay of these two operators is necessary to describe the  $B^- \rightarrow D^+ \pi^- \pi^-$  decay. For all these reasons we will limit our discussion of the weak transitions to these two operators. In particular we will also ignore small contributions proportional to  $V_{ub}$ , as well as perturbative QCD corrections to the Wilson coefficient of the quark operator.

For weak transitions of the form  $H_b \rightarrow S_c$  we consider two weak operators analogous to Eqs. 6 and 7 obtained by replacing  $H_c \rightarrow S_c$ . In principle these

operators have different coefficients than those in Eqs. 6 and 7. However, we estimate all the weak coefficients in naive factorization where the constant  $\beta'_W$  is the same for  $H_b \rightarrow S_c$  and  $H_b \rightarrow H_c$  transitions, and the  $k_H$  and  $k_S$  coefficients are related. For weak transitions involving a  $T$  field, Eq. 6 will not have an analogue in this approximation (the tensor decay constant vanishes [8]). The single weak operator in this case reads,

$$\mathcal{L}_T = ik_T Tr [v_\alpha \bar{T}_v^\alpha \gamma_\mu (1 - \gamma_5) H_v] Tr [\xi^\dagger h \partial^\mu \xi]. \quad (8)$$

The factorization results that we use relate the  $k$  weak constants to the Isgur-Wise functions [14]  $\xi(\omega), \tau_{1/2,3/2}(\omega)$ ,

$$\begin{aligned} \beta'_W &= \frac{G_F V_{cb} V_{ud}}{\sqrt{2}} \frac{1}{12} f_B f_D \sqrt{m_B m_D} B_1 \\ k_H &= -\frac{G_F V_{cb} V_{ud}}{\sqrt{2}} f_\pi^2 \xi(\omega) B_2 \\ k_S &= 2 \frac{G_F V_{cb} V_{ud}}{\sqrt{2}} f_\pi^2 \tau_{1/2}(\omega) B_2 \\ k_T &= \frac{G_F V_{cb} V_{ud}}{\sqrt{2}} \sqrt{3} \tau_{3/2}(\omega) f_\pi^2 B_3. \end{aligned} \quad (9)$$

In order to treat these weak vertices as a phenomenological parametrization we have introduced ‘‘bag factors’’  $B_{1,2,3}$  that are equal to 1 in simple factorization but that we will allow to vary. Numerically we will also use  $\xi(1) = 1$ ,  $\tau_{1/2}(1) \approx 0.25$  and  $\tau_{3/2}(1) \approx 0.35$ ; as well as  $f_B = 191$  MeV and  $f_D = 225$  MeV.

Notice that this framework will describe all the non-resonant diagrams in terms of the same coupling constants as the ‘‘quasi-resonant’’ diagrams. Our strategy is thus to fix as many constants as possible from the on-shell two body decay modes  $B^- \rightarrow D^{**} \pi^-$  and then use these results, supplemented with the HQET description of the strong  $D^{**}$  couplings to predict the three-body decay mode.

### III. $B^- \rightarrow D_s^+ K^- \pi^-$ AND THE $D^{**}$ RESONANCES

We are now in a position to investigate the contribution of the  $D^{**}$  resonances to the  $B^- \rightarrow D_s^+ K^- \pi^-$  process. Our strategy will be to compute the amplitude with the ingredients given in the previous section, schematically splitting it into the two terms pictured in Figure 1. In the limit in which the quasi-resonant states dominate, it is possible to make reliable predictions that depend only on the theory of the strong  $D^{**} DM$  transitions because the weak production vertex and the strong decay vertex factorize, as they do in the narrow width approximation for a resonant channel. The weak transition can then be eliminated in favor of the measured  $B^- \rightarrow D^+ \pi^- \pi^-$ . This approach completely fails as the non-resonant contribution becomes dominant in which case the two decay modes are not directly related. The formalism in the previous section will serve to interpolate between these two extremes, allowing us to explore the sensitivity of our result to the weak couplings.

We begin by computing the  $B^- \rightarrow D_s^+ K^- \pi^-$  amplitude from the 11 diagrams shown in Fig.2. The calculation proceeds as follows. We work in the  $B$  rest frame in

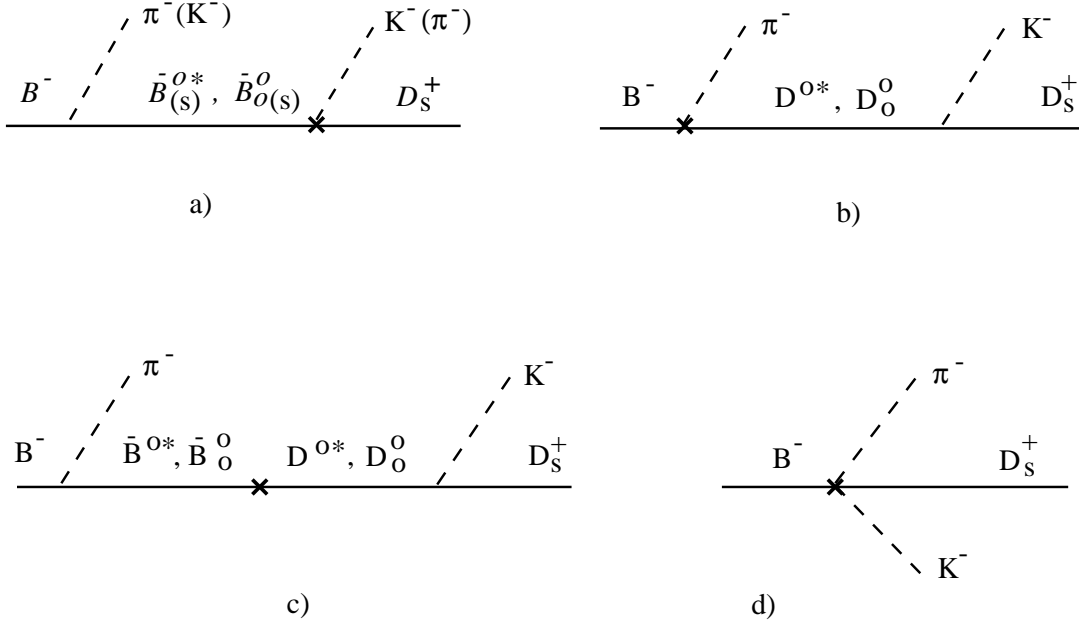


FIG. 2: Diagrams

which the heavy meson has four velocity  $v^\mu = (1, 0, 0, 0)$ . After a weak light meson emission we solve for the velocity of the charmed heavy meson,  $v'$  for  $D_{0,2}^0, D^{0*}$ , using exact kinematics so that the residual momentum in the intermediate heavy meson propagator corresponds exactly to its off-shellness. We then find

$$v' = \left( \frac{m_B - E_\pi}{m_{D_s^+ K^-}}, -\frac{\vec{p}_\pi}{m_{D_s^+ K^-}} \right), \quad \omega = v \cdot v' = \frac{m_B^2 + m_{D_s^+ K^-}^2}{2m_B m_{D_s^+ K^-}}. \quad (10)$$

To determine phenomenological values for our ‘‘bag factors’’ we use the experimental results [2],

$$\begin{aligned} \mathcal{B}(B^- \rightarrow D_0^0 \pi^-) \mathcal{B}(D_0^0 \rightarrow D^+ \pi^-) &= (6.1 \pm 0.6 \pm 0.9 \pm 1.6) \times 10^{-4} \\ \mathcal{B}(B^- \rightarrow D_2^0 \pi^-) \mathcal{B}(D_2^0 \rightarrow D^+ \pi^-) &= (3.4 \pm 0.3 \pm 0.6 \pm 0.4) \times 10^{-4}, \end{aligned} \quad (11)$$

supplemented with the theoretical input for the strong  $D^{**}$  decays as in [11, 15]. For the central values then,

$$\begin{aligned} \mathcal{B}(B^- \rightarrow D_0^0 \pi^-) &= 9.1 \times 10^{-4} \\ \mathcal{B}(B^- \rightarrow D_2^0 \pi^-) &= 8.7 \times 10^{-4}. \end{aligned} \quad (12)$$

The weak decay rates  $B^- \rightarrow D_0^0 \pi^-$  and  $B^- \rightarrow D_2^0 \pi^-$  can be calculated in the above

framework with results,

$$\begin{aligned}\Gamma(B^- \rightarrow D_0^0 \pi^-) &= \frac{E_{D_0^0} E_\pi}{8\pi m_B} \left[ \frac{4\beta'_W \omega_0}{f_\pi} \left\{ 1 + h \frac{m_B + m_{D_s^+ K^-}}{2m_{D_s^+ K^-}} - \frac{k_S E_\pi (m_{D_s^+ K^-} - m_B)}{4\beta'_W \omega m_{D_s^+ K^-}} \right\} \right]^2, \\ \Gamma(B^- \rightarrow D_2^0 \pi^-) &= \frac{k_T^2 E_{D_2} E_\pi (\omega_2^2 - 1)^2 (m_B + m_{D_2})^2}{12\pi^2 m_B f_\pi^2},\end{aligned}\quad (13)$$

where  $\omega_0 = \frac{E_{D_0^0}}{m_{D_0^0}} = 1.362$  and  $\omega_2 = \frac{E_{D_2^0}}{m_{D_2^0}} = 1.306$ . Setting these predictions, Eq. 13, equal to the values in Eq. 12 we find  $B_2$  as a function of  $B_1$ . For our numerics we will use the three pairs  $B_1 = 1, B_2 = 1.13$ ;  $B_1 = 1.308, B_2 = 1$  and  $B_1 = 1.15, B_2 = 1.06$ . From the second line it also follows that  $B_3 = 1.3$ .

We neglect mass splittings between members of a doublet,  $H, S, T$ , but include mass splittings between the different doublets. In addition, we set the pion mass to zero. We find it convenient to evaluate scalar products involving  $v'$  in the  $D_s^+ K^-$  center of mass frame.

All this results in the following amplitudes. The three “quasi-resonant” diagrams (those that contain a  $D_0^0$  meson in Fig.2.b,c) give:

$$\mathcal{M}_S = -\frac{4\beta'_W h \omega}{f_\pi f_K} \frac{v' \cdot q_K}{m_{D_s^+ K^-} - m_{D_0^0}} \left\{ 1 + h \frac{m_B + m_{D_s^+ K^-}}{2m_{D_s^+ K^-}} - \frac{k_S E_\pi (m_{D_s^+ K^-} - m_B)}{4\beta'_W \omega m_{D_s^+ K^-}} \right\}, \quad (14)$$

with  $E_\pi$  evaluated in the  $B$  rest frame. This  $D_0^0$  contribution by itself has an  $M_{D_s^+ K^-}$ -invariant mass distribution shown as the solid line in Fig.3.

There is one diagram with an intermediate tensor  $D_2^{*\star}$  state. It yields an amplitude,

$$\begin{aligned}\mathcal{M}_T &= -\frac{k_T h'}{f_\pi f_K (m_{D_s^+ K^-} - m_{D_2})} \left\{ (\omega + 1) [(q_\pi \cdot q_K - q_\pi \cdot v' q_K \cdot v') (E_K - \omega q_K \cdot v')] \right. \\ &\quad - \frac{1}{3} (m_K^2 - (q_K \cdot v')^2) (E_\pi - \omega q_\pi \cdot v') \Bigg] \\ &\quad - q_\pi \cdot v' \left[ (E_K - \omega q_K \cdot v')^2 - \frac{1}{3} (1 - \omega^2) (m_K^2 - (q_K \cdot v')^2) \right] \Bigg\},\end{aligned}\quad (15)$$

where  $E_{\pi, K}$  are evaluated in the  $B$  rest frame. By itself the  $D_2^0$  contribution has an  $M_{D_s^+ K^-}$ -invariant mass distribution shown as the dashed line in Fig.3.

Finally there are 8 “non-resonant” diagrams that do not involve a  $D^{*\star}$  intermediate state. The 5 diagrams from Fig.2.a,d give:

$$\begin{aligned}\mathcal{M}_{\text{other}} &= -\frac{4\beta'_W \omega}{f_\pi f_K} \left( 1 - \frac{h q_\pi \cdot v'}{m_{D_s^+ K^-} - m_B} + \frac{h k_S (m_B - m_D) q_\pi \cdot q_D}{4\beta'_W \omega m_B m_D} \right) \\ &\quad + \frac{4\beta'_W g (q_\pi \cdot q_D - q_\pi \cdot v' q_D \cdot v')}{f_\pi f_K (m_{D_s^+ K^-} - m_B) m_D} \\ &\quad - \frac{2g k_H m_B (q_\pi \cdot q_K - q_\pi \cdot v_{B_s^*} q_K \cdot v_{B_s^*})}{f_\pi f_K (m_K^2 - 2p_B \cdot q_K)} \left( \frac{2q_D \cdot q_\pi}{m_B m_D} + \frac{m_D}{m_B} + 1 \right),\end{aligned}\quad (16)$$

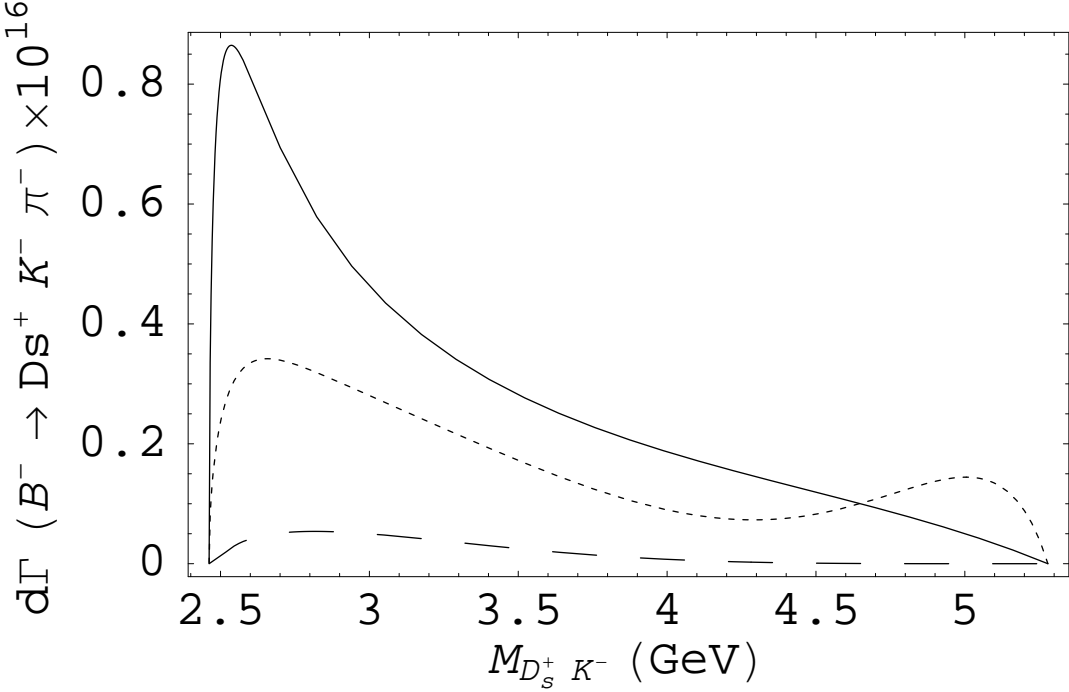


FIG. 3:  $M_{D_s^+ K^-}$  invariant mass distribution for  $B_1 = 1$ ,  $B_2 = 1.13$  for: a) diagrams involving a  $D_0^0$  (solid line); b) diagrams involving a  $D_2^0$  (dashed line) and c) all other diagrams (dotted line). Interference terms between (a), (b), and (c) are not shown.

where

$$v_{B_s^*} = \left( \frac{m_B - E_K}{m_{D_s^+ \pi^-}}, -\frac{\vec{p}_K}{m_{D_s^+ \pi^-}} \right). \quad (17)$$

The remaining 3 diagrams from Fig.2.b,c with a  $D^{0*}$  intermediate state give:

$$\begin{aligned} \mathcal{M}_{D^*} = & -\frac{4g\beta'_W}{f_\pi f_K(m_{D_s^+ K^-} - m_{D^*})} \left\{ 1 - \frac{k_H}{4\beta'_W} q_\pi \cdot v' \right\} (E_K - \omega q_K \cdot v') \\ & + \frac{g(q_\pi \cdot q_K - q_\pi \cdot v' q_K \cdot v')}{f_\pi f_K(m_{D_s^+ K^-} - m_{D^*})} \left\{ -k_H(\omega + 1) + \frac{4g\beta'_W}{m_{D_s^+ K^-} - m_{B^*}} \right\}. \end{aligned} \quad (18)$$

All eight “non-resonant” diagrams give a partial contribution to the  $M_{D_s^+ K^-}$  invariant mass distribution shown as the dotted line in Figure 3.

We now show the full result obtained by adding all contributions. This is not equal to the sum of the three curves in Figure 3 because that decomposition ignored the interference between different terms. To obtain the total rate it is necessary to know the relative sign of the coupling  $h'$ . Since this is not known we present results for both signs. With a positive  $h'$  we obtain a total  $\mathcal{B}(B^- \rightarrow D_s^+ K^- \pi^-) = 4.8 \times 10^{-5}$  and with a negative  $h'$  we find  $\mathcal{B}(B^- \rightarrow D_s^+ K^- \pi^-) = 9.2 \times 10^{-5}$ . The corresponding  $M_{D_s^+ K^-}$  invariant mass distributions are shown in Fig.4 for three values of  $B_1$  and  $B_2$  as described earlier.

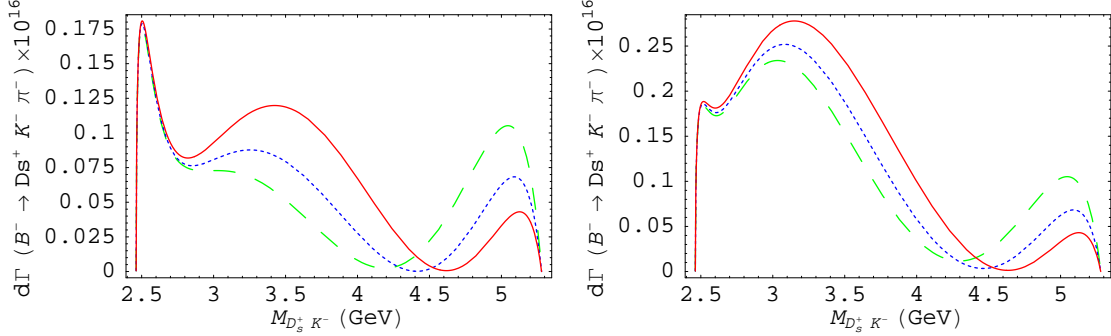


FIG. 4:  $M_{D_s^+ K^-}$  invariant mass distributions with  $B_1 = 1$ ,  $B_2 = 1.13$  (solid),  $B_1 = 1.15$ ,  $B_2 = 1.06$  (dotted),  $B_1 = 1.308$ ,  $B_2 = 1$  (dashed) for (a)  $h' = 0.5 \text{ GeV}^{-1}$  and (b)  $h' = -0.5 \text{ GeV}^{-1}$ .

#### IV. DISCUSSION

##### A. Dependence on the parametrization of the weak vertex

In Figure 4 we have already presented results for three different pairs of values for  $B_1$  and  $B_2$ . These correspond to different parametrizations for the weak vertex that reproduce the central value of the two body decay rates. We see from that figure that the variations are not large. We now explore in more detail the dependence of the total rate on these parameters. To this end we first normalize the total decay rate obtained in the previous section to the rate  $B^- \rightarrow D_0^0 \pi^-$  calculated in Eq. 13. We then plot this ratio as a function of the “bag factor”  $B_1$  while adjusting  $B_2$  in such a way that  $B^- \rightarrow D_0^0 \pi^-$  remains fixed to its experimental (central) value in Figure 5a.

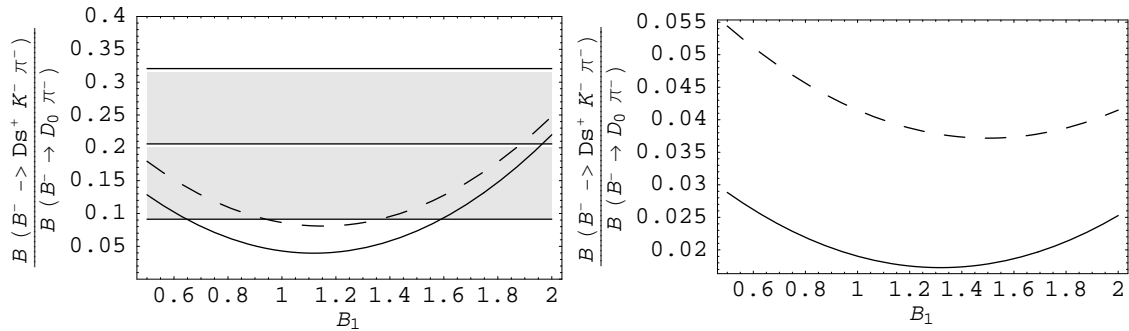


FIG. 5: Ratio of two modes as a function of  $B_1$  factor for: a) full kinematic range; and b)  $M_{D_s^+ K^-} \leq M_{D_0^0} + 3\Gamma_{D_0^0} \sim 3.2 \text{ GeV}$ . The horizontal lines in (a) show the  $1-\sigma$  range from the BaBar measurement [1]. In both cases the solid line corresponds to  $h' > 0$  and the dashed line to  $h' < 0$ .

We see that the ratio changes by about a factor of four when we span the value of  $B_1$  from 1/2 to 2 (recall  $B_1 = 1$  in naive factorization). This variation indicates

that our prediction for the full rate  $\mathcal{B}(B^- \rightarrow D_s^+ K^- \pi^-)$  is not robust over the full kinematic range in that the process is not dominated by the  $D_0^{**}$  quasi-resonance. In the figure we also show the  $1-\sigma$  band from the BaBar measurement [1] and we see that our prediction for the total rate is a bit low for values of  $B_1$  close to one.

Following our general discussion, we might expect to do better if we limit the range for  $m_{D_s^+ K^-}$  to values closer to the physical  $M_{D_0^0}$  mass, since this would enhance the relative contribution of the “quasi-resonance”. For illustration we repeat the above exercise including only the partial branching ratio  $\mathcal{B}(B^- \rightarrow D_s^+ K^- \pi^-)$  from the region  $M_{D_s^+ K^-} \leq M_{D_0^0} + 3\Gamma_{D_0^0} \sim 3.2$  GeV. We show these results in Fig.5b. We notice a significant improvement in the form of reduced dependence of our prediction on the parametrization of the weak vertex. In particular the dependence is very weak for “bag factors” within 20% of the naive factorization.

## B. Angular distributions

We now turn our attention to angular distributions and the additional information they provide. In particular, by studying the angular distribution  $d\Gamma(B^- \rightarrow D_s^+ K^- \pi^-)/d\cos\theta$  for the angle  $\theta$  between the momenta of the pion and the kaon in the  $D_s^+ K^-$  center of mass frame one can extract the amplitudes with different angular momentum. This frame would correspond to the rest frame of the  $D^{**}$  if it were produced as a physical intermediate state, and this is the angular distribution that would normally be used to determine the spin of the resonance. In  $B^- \rightarrow D_s^+ K^- \pi^-$  there is no resonance in the physical region, but we expect the different contributions to the rate to exhibit different angular distributions depending on the virtual intermediate state. This is made evident by rewriting the amplitudes in the  $D_s^+ K^-$  center of mass frame. We find that the total amplitude in this frame can be written as a linear superposition of Legendre polynomials in  $\cos\theta_{K-\pi^-}$  (the angle between the  $K^-$  and  $\pi^-$  momenta in the  $D_s^+ K^-$  center of mass frame),

$$\mathcal{M}(B^- \rightarrow D_s^+ K^- \pi^-) = \mathcal{M}_0 P_0(\cos\theta_{K-\pi^-}) + \mathcal{M}_1 P_1(\cos\theta_{K-\pi^-}) + \mathcal{M}_2 P_2(\cos\theta_{K-\pi^-}) + \dots \quad (19)$$

With sufficient statistics it should be possible to fit the observed angular distribution to a form

$$\frac{d\Gamma(B^- \rightarrow D_s^+ K^- \pi^-)}{\cos\theta_{K-\pi^-}} \sim |\mathcal{M}_0|^2 + |\mathcal{M}_1|^2 \cos^2\theta_{K-\pi^-} + |\mathcal{M}_2|^2 \frac{(3\cos^2\theta_{K-\pi^-} - 1)^2}{4} \quad (20)$$

and in this way extract these three components of the branching ratio. They correspond to the  $D_s^+ K^-$  system having angular momentum 0, 1 or 2 respectively.

Within our framework, we find for the partial amplitudes,

$$\begin{aligned}
\mathcal{M}_0 &= -\frac{4\beta'_W h E_K^* \omega_0}{f_\pi f_K (m_{D_s^+ K^-} - m_{D_0^0})} \left\{ 1 + h \frac{m_{D_s^+ K^-} + m_B}{2m_{D_s^+ K^-}} \right. \\
&\quad - \frac{k_S E_\pi^*}{4\omega_0 \beta'_W} \left[ \frac{m_{D_s^+ K^-} - m_B}{m_B} - \frac{E_D^* (m_B - m_D) (m_{D_s^+ K^-} - m_{D_0^0})}{E_K^* m_B m_D} \right] \\
&\quad \left. - \frac{E_\pi^* (m_{D_s^+ K^-} - m_{D_0^0})}{E_K^* (m_{D_s^+ K^-} - m_B)} \right\} - \frac{4\beta'_W \omega}{f_\pi f_K} + a_0 \\
\mathcal{M}_1 &= \frac{4\beta'_W g |\vec{q}_\pi| |\vec{q}_K|}{f_\pi f_K (m_{D_s^+ K^-} - m_{D^{*0}})} \left\{ \frac{1}{m_B} - \frac{g}{m_{D_s^+ K^-} - m_{B^*}} + \frac{k_H}{4\beta'_W} \frac{m_{D_s^+ K^-} + m_B}{m_B} \right. \\
&\quad + \frac{m_{D_s^+ K^-} - m_{D^{*0}}}{(m_{D_s^+ K^-} - m_{B^*}) m_D} - \frac{h k_S}{4\beta'_W g} \frac{(m_B - m_D) (m_{D_s^+ K^-} - m_{D^{*0}})}{m_B m_D} \left. \right\} + a_1 \\
\mathcal{M}_2 &= \frac{2 h' k_T |\vec{q}_\pi|^2 |\vec{q}_K|^2 (m_{D_s^+ K^-} + m_B)}{3 f_\pi f_K (m_{D_s^+ K^-} - m_{D_0^0}) m_B^2} + a_2,
\end{aligned} \tag{21}$$

where the starred energies are evaluated in the  $D_s^+ K^-$  center of mass frame. In Eq. 21 we have shown explicitly the contributions to the  $J = 0, 1, 2$  amplitudes from the diagrams with an intermediate  $D_0^0$ ,  $D^{*0}$  and  $D_2^0$  respectively. Additional contributions arise from the non-resonant diagrams, in particular the diagram in which a  $B_s^{0*}$  is exchanged with the  $K^-$  connected to the  $B$  vertex and the  $\pi^-$  connected to the  $D_s^+$  vertex contributes to all values of angular momentum. We denote its projections into  $J = 0, 1, 2$  by  $a_0$ ,  $a_1$ ,  $a_2$  and evaluate these contributions numerically. We show this decomposition in Fig.6 for  $B_1 = 1$ ,  $B_2 = 1.13$  as a function of  $D_s^+ K^-$  invariant mass.

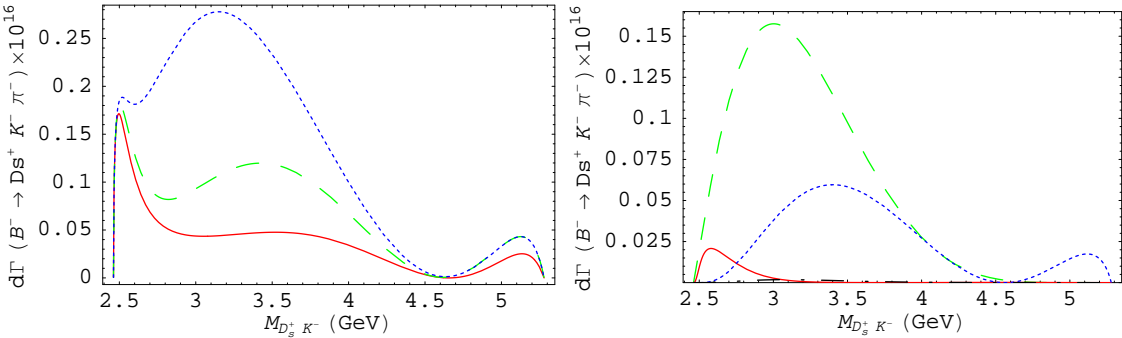


FIG. 6: Contributions to the decay rate from different spin amplitudes for  $B_1 = 1$ ,  $B_2 = 1.13$ : a)  $M_0$  (solid) and total (dashed and dotted) for different  $h'$  sign ; and b)  $M_1$  (dotted),  $M_2$  for negative  $h'$  (dashed) and positive  $h'$  (solid), and higher spins (dot-dashed).

As can be seen from Figure 6 this analysis yields substantially more information. The large difference in the total contribution for different signs of  $h'$  indicates a large interference between the amplitude mediated by  $D_2^0$  and  $a_2$ . Numerically, we find

$$\frac{\Gamma_2(B^- \rightarrow D_s^+ K^- \pi^-)}{\Gamma(B^- \rightarrow D_2^0 \pi^-)} \approx (0.24h' - 0.085)^2. \tag{22}$$

An extraction of  $|\mathcal{M}_2|^2$  from an angular analysis would then determine the relative sign of  $h'$ . For negative  $h'$  this contribution is large as seen in Figure 6, whereas for positive  $h'$  it is much smaller.

We can also see from the figure that the spin one contribution is not negligible and is most important for intermediate values of  $m_{D_s^+ K^-}$ . Contributions from spin higher than two are negligible as seen in the Figure 6b. To further quantify these contributions we calculate the respective partial branching ratios, finding (in a self-evident notation),

$$\begin{aligned}
\mathcal{B}_0(B^- \rightarrow D_s^+ K^- \pi^-) &= 2.6 \times 10^{-5} \\
\mathcal{B}_1(B^- \rightarrow D_s^+ K^- \pi^-) &= 1.7 \times 10^{-5} \\
\mathcal{B}_2(B^- \rightarrow D_s^+ K^- \pi^-) &= 4.0 \times 10^{-5} \quad h' < 0 \\
&\quad = 1.6 \times 10^{-6} \quad h' > 0 \\
\mathcal{B}_{J>2}(B^- \rightarrow D_s^+ K^- \pi^-) &= 4.2 \times 10^{-7}.
\end{aligned} \tag{23}$$

Finally we can repeat the exercise leading to Figure 5 to determine the dependence of the rate on the parametrization of the  $D_0^0$  weak vertex limiting the analysis to the spin 0 contribution. We show this result in Figure 7. There is still a large

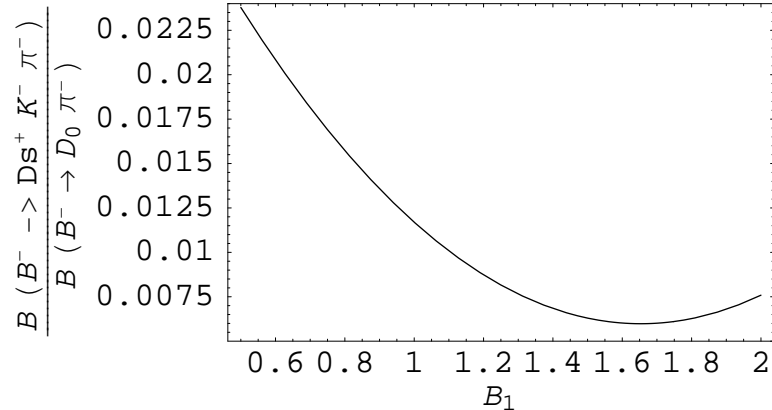


FIG. 7: Ratio of two modes as a function of  $B_1$  factor for the range  $M_{D_s^+ K^-} \leq M_{D_0^0} + 3\Gamma_{D_0^0} \sim 3.2$  GeV including only the  $\mathcal{M}_0$  contribution.

dependence on the parametrization of the weak vertex as the ratio varies by a factor of three in the range  $0.5 < B_1 < 2$ . This is not surprising as Eq. 21 indicates there is a large non-resonant contribution to spin 0, which is not dominated by the  $D_0^0$ .

## V. $B^- \rightarrow D_0^0 \pi^- \rightarrow D_0^* \gamma \pi^-$

We end this paper with a brief discussion of the radiative decay  $D_0^0 \rightarrow D_0^* \gamma$ . This partial mode can be studied more reliably in the chain  $B^- \rightarrow D_0^0 \pi^- \rightarrow D_0^* \gamma \pi^-$

because in this case the physical resonance dominates and the approximation in which the weak production of  $D_0^0$  and its radiative decay factorize should be reliable.

The production rate  $B^- \rightarrow D_0^0\pi^-$  was already obtained in Eq.12, and the subsequent radiative decay of the  $D_0^0$  can be readily extracted from the vertices in Ref. [13] (see Eqs. 14, 15, A4 in that reference),

$$\Gamma(D_0^0 \rightarrow D^{0*}\gamma) = (e\mu_D^S)^2 \cdot \frac{E_\gamma^3}{m_{D_0^0}} \cdot \frac{E_{D^{0*}}}{4\pi} \approx 0.09\text{MeV}, \quad (24)$$

where we used the result  $\mu_D^S = \frac{2e_c\tau^{1/2}(1)}{m_c} + \frac{e_u}{\Lambda'_{1/2}} \approx 0.75\text{GeV}^{-1}$  with input parameters discussed in Ref. [13].

Using  $\Gamma_{D_0^0} = 276\text{MeV}$ , we find  $\mathcal{B}(D_0^0 \rightarrow D^{0*}\gamma) = 3.3 \times 10^{-4}$ . With sufficient statistics to observe this mode it will then be possible to extract the coupling  $\mu_D^S$ .

## VI. CONCLUSIONS

We have analyzed the mode  $B^- \rightarrow D_s^+ K^- \pi^-$  using HQET to parametrize “quasi-resonant” and non-resonant contributions. With the aid of angular analysis it should be possible to extract the contributions of virtual intermediate states with spin 0, 1, or 2 leading to the  $D_s^+ K^-$  final state.

The spin zero partial rate receives a large but not dominant contribution from the  $D_0^0$  intermediate state. This means that it is not possible to test the  $D_0^0 D_s^+ K^-$  vertex in a model independent way. However, we have seen that the HQET description gives a picture for this decay that can be tested qualitatively at least.

The spin one contribution is surprisingly large as it is dominated by an intermediate  $D^{*0}$  with a mass significantly below threshold. This reinforces the conclusion that the decay is not dominated by the  $D^{**}$  resonances although they play an important role.

The spin two contribution is perhaps the most interesting one. We find that it could be quite large or quite small depending on the sign of the strong coupling constant  $h'$ . A study of this contribution should provide strong evidence for the sign of this coupling.

Given the large  $m_b - m_c$  mass difference we do not expect the momentum expansion to describe the weak decay quantitatively. However, we have provided a mixed framework that uses HQET to describe strong transitions and a naive factorization that describes weak transitions in terms of a few phenomenological parameters. This framework results in a qualitative description for this decay mode that can be used to compare with experiment and perhaps extract some information on the signs and the  $SU(3)$  properties of the strong vertices.

## Acknowledgments

This work was supported in part by DOE under contract number DE-FG02-01ER41155. We thank Vitaly Eges and Soeren Prell for useful discussions.

---

- [1] “Study of B decays to open charm final state with the BaBar experiment” by Giovanni Calderini from the BaBar Collaboration, ICHEP 06,Moscow. <http://ichep06.jinr.ru/session.asp?sid=8>
- [2] K. Abe *et al.* [Belle Collaboration], Phys. Rev. D **69**, 112002 (2004) [arXiv:hep-ex/0307021].
- [3] M. B. Wise, Phys. Rev. D **45**, 2188 (1992).
- [4] T. M. Yan, H. Y. Cheng, C. Y. Cheung, G. L. Lin, Y. C. Lin and H. L. Yu, Phys. Rev. D **46**, 1148 (1992) [Erratum-ibid. D **55**, 5851 (1997)].
- [5] G. Burdman and J. F. Donoghue, Phys. Lett. B **280**, 287 (1992).
- [6] Aneesh V. Manohar and Mark B. Wise, “Heavy quark physics” (2000). Cambridge Monographs on Particle Physics, Nuclear Physics, and Cosmology.
- [7] A. F. Falk, Nucl. Phys. B **378**, 79 (1992).
- [8] R. Casalbuoni, A. Deandrea, N. Di Bartolomeo, R. Gatto, F. Feruglio and G. Nardulli, Phys. Rept. **281**, 145 (1997) [arXiv:hep-ph/9605342].
- [9] U. Kilian, J. G. Korner and D. Pirjol, Phys. Lett. B **288**, 360 (1992).
- [10] A. F. Falk and M. E. Luke, Phys. Lett. B **292**, 119 (1992) [arXiv:hep-ph/9206241].
- [11] F. Jugeau, A. Le Yaouanc, L. Oliver and J. C. Raynal, Phys. Rev. D **72**, 094010 (2005) [arXiv:hep-ph/0504206].
- [12] H. Georgi, “Weak Interactions And Modern Particle Theory,” Benjamin/Cummings Pub. Co., Menlo Park, Calif. 1984.
- [13] O. Antipin and G. Valencia, Phys. Rev. D **74**, 054015 (2006) [arXiv:hep-ph/0606065].
- [14] N. Isgur and M. B. Wise, Phys. Rev. D **43**, 819 (1991).
- [15] H. Y. Cheng and C. K. Chua, Phys. Rev. D **74**, 034020 (2006) [arXiv:hep-ph/0605073].